

Abstract

Different methods of determining formation rates of 3 nm particles are compared, basing on analysis of simulated data, but the results are valid for analyses of experimental particle size distribution data as well. The study shows that the method of determining formation rates indirectly from measured number concentration data of 3–6 nm particles is generally in good agreement with the theoretical calculation with a systematic error of 0–20%. While this is often accurate enough, a simple modification to the approximative equation for the formation rate is recommended. Additionally, the temporal connection between the concentration of the nucleating vapour and the formation rate is studied. It is concluded that the often used power-law connecting these two is inaccurate.

1 Introduction

Formation of new particles by nucleation and their subsequent growth to larger sizes have been observed to take place frequently and almost everywhere in the Earth's atmosphere (Kulmala et al., 2004; Kulmala and Kerminen, 2008). Model studies indicate that nucleation is a dominant source of new particles (Spracklen et al., 2006; Yu and Luo, 2009) and a very important source of cloud condensation nuclei and cloud droplets (Spracklen et al., 2008; Makkonen et al., 2009; Merikanto et al., 2009; Pierce and Adams, 2009) in the global atmosphere.

From a theoretical point of view, atmospheric new-particle formation is driven by the nucleation rate, i.e. the formation rate of critical clusters of 1–2 nm in diameter (e.g. Kulmala et al., 2007). The nucleation rate is, however, a problematic quantity to deal with. Firstly, in spite of the recent progress in measuring atmospheric clusters and nanometer-size particles (Sipilä et al., 2008; Iida et al., 2009; Lehtipalo et al., 2009; Manninen et al., 2009), accurate measurements of atmospheric nucleation rates are impossible at the moment. Secondly, few large-scale atmospheric models extend their

A numerical comparison of formation rates

H. Vuollekoski et al.

Title Page

Abstract

Introduction

Conclusions

References

Tables

Figures



Back

Close

Full Screen / Esc

Printer-friendly Version

Interactive Discussion



size distribution down to 1 nm needed to simulate the nucleation process. Atmospheric new-particle formation is therefore usually handled by using the concept of the “apparent” particle formation rate (e.g. Kerminen and Kulmala, 2002), which refers to the formation rate of particles of a few nm (typically 3 nm) in diameter.

5 The connection between the nucleation rate and apparent particle formation rate has been studied quite actively during the recent years (e.g. Kerminen et al., 2004; McMurry et al., 2005; Lehtinen et al., 2007; Anttila et al., 2010). Much less attention has been put on investigating how accurately the particle formation rate can be determined from atmospheric measurements, how sensitive this rate is to the applied analysis method and the underlying assumptions, and how this rate should be related to the nucleation rate in practice. Such information would be extremely valuable when testing current nucleation theories against field or laboratory measurement data, or when evaluating the performance of nucleation parameterizations in large-scale atmospheric models.

15 The goal of this paper is to address some of the issues raised above with help of an aerosol dynamics model. By using simulated, rather than measured, data, it is possible to investigate the particle formation rate and related quantities in a controlled system and without the problems inherent to experimental data. The latter include the diurnal evolution of the atmospheric boundary layer, rapid changes in air masses transported to the measurement site, and the often poorly-quantified time delay between nucleation and apparent particle formation. Since we treat our simulation data as it were traditional field measurement data, our results should be valid for analyses of experimental data as well, at least within the numerical and physical accuracy of the applied aerosol dynamics model.

A numerical comparison of formation rates

H. Vuollekoski et al.

Title Page

Abstract

Introduction

Conclusions

References

Tables

Figures



Back

Close

Full Screen / Esc

Printer-friendly Version

Interactive Discussion



2 Theory

The time evolution of particle size distribution is described by the (simplified) continuous general dynamic equation (e.g. Seinfeld and Pandis, 2006)

$$\begin{aligned} \frac{\partial n(v,t)}{\partial t} = & \frac{1}{2} \int_0^v K(v-q,q)n(v-q,t)n(q,t)dq - n(v,t) \int_0^\infty K(q,v)n(q,t)dq \\ & - \frac{\partial}{\partial v}[(\rho_k - \gamma_k)v_1 n(v,t)] + J_{\text{nuc}}(t)\delta(v - v_0) + S(v,t) - R(v,t), \end{aligned} \quad (1)$$

where $n(v,t) = \partial N / \partial v$ is the particle volume distribution function, v is particle volume, t is time, N is the cumulative number concentration of particles, $K(v,v')$ is the coagulation coefficient between particles of volumes v and v' , ρ_k and γ_k are the rates at which a k -mer gain or lose a monomer due to condensation or evaporation, v_1 is the volume of the condensing/evaporating monomer, J_{nuc} is the nucleation rate, δ is the delta function, v_0 is the volume of nucleated particles, and S and R represent additional sources and losses. Note that the quantities are defined here in the continuous volume sense, while in this paper we investigate both continuous and discrete quantities.

In this paper, the particles are assumed to be spherical, and so it is more practical to use particle diameter instead of volume. While it can be defined at any size, let us, for the remainder of this paper, assume that by formation rate we mean it at the most widely studied diameter $D_p = 3$ nm, unless stated otherwise. Even though recent measurements have been able to estimate particle formation rates at as low as 2 nm (Kulmala et al., 2007; Manninen et al., 2009), only a fraction of particle size distribution data extends to below 3 nm. Since the mathematical relations used in this paper are applicable at any size, a more conventional size of 3 nm is also more meaningful from the point of view of this study, as the diameter change from nucleation is larger than with 2 nm particles, allowing for more time for e.g. coagulation.

Particles of 3 nm in diameter may be formed due to condensational growth of particles from below 3 nm, shrinkage of particles due to evaporation from above 3 nm, and

A numerical comparison of formation rates

H. Vuollekoski et al.

Title Page

Abstract

Introduction

Conclusions

References

Tables

Figures

◀

▶

◀

▶

Back

Close

Full Screen / Esc

Printer-friendly Version

Interactive Discussion



self-coagulation of particles smaller than 3 nm. Since nuclei self-coagulation is important at high nucleation rates only, it may be neglected in typical atmospheric conditions (e.g. Anttila et al., 2010). While keeping these assumptions in mind, we denote the formation rate of particles at 3 nm by J_3 . In words, this signifies the flux of particle concentration on “diameter axis” at exactly 3 nm in size. An equation for this can then be written as

$$J_3 = n_3 \times GR_3 = \left. \frac{\partial N}{\partial D_p} \right|_3 GR_3, \quad (2)$$

where $n_3 = \left. \frac{\partial N}{\partial D_p} \right|_3$ is from now on the size distribution function at 3 nm, $GR_3 = \left. \frac{dD_p}{dt} \right|_3$ is the growth rate of particles at 3 nm, which represents the term $(p_k - \gamma_k)v_1$ in Eq. (1): the growth due to condensation and shrinkage due to evaporation.

Note that in a stationary situation $\left. \frac{\partial N}{\partial t} \right|_3 = 0$, but according to Eq. (2) the formation rate J_3 need not equal zero.

3 Methods

3.1 Formation rate of 3 nm particles

Unfortunately, the presented definition of formation rate, Eq. (2), is difficult to apply in practise. In a sectional aerosol dynamics model, the formation rate can be estimated by approximating the partial derivative, and interpolating (if needed) over particle diameter, to get

$$J_3 = \left. \frac{\Delta N}{\Delta D_p} \right|_3 \times GR_3, \quad (3)$$

where ΔD_p is the width of the section centered around 3 nm particles, and ΔN is the particle concentration in the corresponding section. Note that since the efficacy of

A numerical comparison of formation rates

H. Vuollekoski et al.

Title Page

Abstract

Introduction

Conclusions

References

Tables

Figures

◀

▶

◀

▶

Back

Close

Full Screen / Esc

Printer-friendly Version

Interactive Discussion



coagulation decreases with increasing particle size, particles between the lower limit and the middle of a size section are scavenged more effectively than particles closer to the upper limit of the same size section. This means that the J_3 calculated with Eq. (3) actually corresponds to formation rate at a size slightly larger than the center of the bin. With typical atmospheric particle concentrations, however, this effect becomes important only if the size resolution of the data is very coarse, and, in practise, below 2 nm.

In this study we used the University of Helsinki Multicomponent Aerosol model (UHMA, Korhonen et al., 2004) to produce the data for analysis. UHMA is a size segregated sectional box model that includes all basic aerosol dynamical processes. A model has the advantage over atmospheric measurements that anything modeled can also be output and saved for further analysis. In this study we used a 1 min output time resolution with 60 fixed size sections divided logarithmically between particle diameters 1.5–1000 nm. New particles were formed via the sulphuric acid induced cluster activation (Kulmala et al., 2006) at the smallest model section.

State-of-the-art instruments, on the other hand, lack detailed resolution in both time and size. In general, noise and other experimental errors decrease their accuracy. In case of an instrument that divides particles according to size channels, such as the differential mobility particle sizer (DMPS, e.g. Aalto et al., 2001), one could in principle directly apply Equation 3. However, since the DMPS has a lower size limit at 3 nm, it is practically impossible to determine GR_3 accurately from DMPS size distribution data. Instead, an average growth rate can be estimated e.g. from the rate of change in mode diameter of (roughly) 3–7 nm particles. Also, using data originating only from one instrument channel is unreliable. Therefore, it is practical to determine the formation rate via the number concentration of e.g. 3–6 nm particles, N_{3-6} . By integrating Eq. (1) over 3–6 nm, and neglecting the self-coagulation as well as other small terms, we get a balance equation

$$\frac{\partial N_{3-6}}{\partial t} = GR_3 \times n_3 - GR_6 \times n_6 - CoagS_{3-6} \times N_{3-6}, \quad (4)$$

A numerical comparison of formation rates

H. Vuollekoski et al.

[Title Page](#)[Abstract](#)[Introduction](#)[Conclusions](#)[References](#)[Tables](#)[Figures](#)[⏪](#)[⏩](#)[◀](#)[▶](#)[Back](#)[Close](#)[Full Screen / Esc](#)[Printer-friendly Version](#)[Interactive Discussion](#)

where the terms on the right-hand-side represent growth from below 3 nm, growth past 6 nm and coagulation loss within 3–6 nm, respectively. CoagS_{3-6} is the mean coagulation sink experienced by 3–6 nm particles (Kulmala et al., 2001). To facilitate its calculation, this range of coagulation sinks may be approximated by just CoagS_4 , as 4 nm is close to the geometric mean of 3–6 nm. By rearranging, approximating the differentials by finite differences, approximating GR_6 by the average growth rate of 3–7 nm particles GR_{3-7} , and denoting the first term on the right-hand-side of Eq. (4) by J_3 , we get (e.g. Sihto et al., 2006; Riipinen et al., 2007)

$$J_3 = \frac{\Delta N_{3-6}}{\Delta t} + \text{CoagS}_4 \times N_{3-6} + \frac{\text{GR}_{3-7}}{6 \text{ nm} - 3 \text{ nm}} \times N_{3-6}. \quad (5)$$

We will use this equation as the measurement perspective, while all the analysis in this paper is still performed on simulated data.

Several approximations were made to arrive at Eq. (5), but it is unclear what is the magnitude of error in this approach. In experimental observations, number concentrations are usually directly measured, while the coagulation sink and growth rate are calculated basing on them. Since the growth rate may be a several-hour average, it is a potential source of error. On the other hand, the size resolution of the measuring instrument might be inadequate to give an accurate estimate of particle concentration in exactly 3–6 nm. We will calculate N_{3-6} by both approximating it as a sum of particle concentrations within bins in size region 3–6 nm, and using more accurate numerical integration. We will also try several other particle size ranges in the application of Eq. (5).

3.2 Connection between the particle formation rate and the precursor vapor concentrations

Several studies have found a simple, empirical relation between the atmospheric sulphuric acid concentration and the formation rate of 3 nm particles (Weber et al., 1996;

A numerical comparison of formation rates

H. Vuollekoski et al.

[Title Page](#)[Abstract](#)[Introduction](#)[Conclusions](#)[References](#)[Tables](#)[Figures](#)[⏪](#)[⏩](#)[◀](#)[▶](#)[Back](#)[Close](#)[Full Screen / Esc](#)[Printer-friendly Version](#)[Interactive Discussion](#)

Sihto et al., 2006; Riipinen et al., 2007; Kuang et al., 2008; Paasonen et al., 2010):

$$J_3(t) \sim [\text{H}_2\text{SO}_4]^p(t - \Delta t(t)). \quad (6)$$

Here, Δt is the time delay between nucleation (as traced by sulphuric acid concentration) and apparent particle formation, and the value of the exponent p provides information about the nucleation mechanism (e.g. McMurry and Friedlander, 1979; Kulmala et al., 2006). Practically all field measurements conducted so far, as well as the recent laboratory experiments (e.g. Metzger et al., 2010; Sipilä et al., 2010), suggest p to be within the range of 1–2.

Application and interpretation of Eq. (6) is complicated by two things. Firstly, the nucleation and early growth of particles seem to be influenced not only by sulphuric acid but also by some low-volatile organic vapors (Paasonen et al., 2009, 2010; Metzger et al., 2010). Secondly, the concentrations of these vapors are expected to have a substantial temporal variability mainly due to the diurnal cycle of the photochemical activity driving their gas-phase production. As a result, the particle growth rate and the time delay, Δt , are expected to vary in time as well. Here, we will use the method described by Vuollekoski et al. (2010) to calculate this temporal behaviour of the time delay in a sectional model, approximated by

$$\Delta t(t) = \sum_{k|D_{p,k} < 3 \text{ nm}} \frac{(D_{p,k} - D_{p,k-1})}{\overline{\text{GR}}_k(t)}, \quad (7)$$

where $D_{p,k}$ is the diameter of size section k and $\overline{\text{GR}}_k(t)$ is the growth rate averaged over the time that it takes for the particles to grow from section $k - 1$ to section k , starting from time t . We will use this time-dependent time delay to investigate Eq. (6) in more detail.

A numerical comparison of formation rates

H. Vuollekoski et al.

Title Page

Abstract

Introduction

Conclusions

References

Tables

Figures

⏪

⏩

◀

▶

Back

Close

Full Screen / Esc

Printer-friendly Version

Interactive Discussion



4 Results and discussion

4.1 Comparison of different methods for estimating the formation rate

We calculated the formation rate of 3 nm particles by using Eqs. (3) and (5) (the “theoretical” and “measured” formation rates, respectively) from simulated new particle formation event data. The vapour concentrations used in the simulation are presented in Fig. 1, and a surface plot of the simulated particle size distribution data is presented in Fig. 2. The “measured” formation rate was determined in two ways: by using a time dependent but size-averaged growth rate for 3–7 nm particles, and by using a single value for the growth rate estimated visually from the particle size distribution plot (3 nm/h). The formation rates are plotted as functions of time in Fig. 3. With this parameterization, the “measured” formation rate overestimates the theoretical one by 10–15%. Nevertheless, the two equations are in a surprisingly good agreement, especially when the growth rate was visually estimated.

The terms from the Eq. (5) are plotted for comparison in Fig. 4. One might suggest that a poorly estimated growth rate could make the “measured” formation rate deviate significantly from the “theoretical” one. The magnitude and order of importance of different terms depend on the conditions of the new particle formation event. For an example, a more abundant background of pre-existing particles would amplify the coagulation sink and consequently reduce the number concentration of 3–6 nm particles, affecting all terms in Eq. (5), but due to the more direct effect of the background concentration on the coagulation sink, the coagulation term would increase the most. Therefore, the error from using Eq. (5) instead of Eq. (3) might increase.

We performed some sensitivity checks on the ratio of different methods of determining the formation rate, Eqs. (3) and (5), by varying the cluster activation coefficient (Kulmala et al., 2006) used in nucleation, the concentration of condensing (particle-growing) vapour and the number concentration of background particles. The results are presented in Table 1. The study showed that changing the activation coefficient has very little effect on the ratio. On the other hand, if the vapour concentration was

A numerical comparison of formation rates

H. Vuollekoski et al.

Title Page

Abstract

Introduction

Conclusions

References

Tables

Figures

◀

▶

◀

▶

Back

Close

Full Screen / Esc

Printer-friendly Version

Interactive Discussion



increased, the growth rate would be higher and more particles would grow to 3–6 nm before being coagulated. Because the loss due to coagulation is most significant for particles below 3 nm, this would decrease the importance of the coagulation term, which would then again bring the ratio between formation rates closer to unity. Similarly, if the background particle concentration was decreased, the coagulation term would weaken, and Eqs. (3) and (5) would be more consistent.

In deriving Eq. (5) from Eq. (4), several approximations were made. We modified the analysis to be more accurate, and the results are presented in Table 2. For example, the actual coagulation sink of 3–6 nm particles was approximated by that of 4 nm particles, and by comparing these, we found that the approximation causes an error of about 8% in the value of CoagS_{3-6} . By applying this improved coagulation sink in Eq. (5), the ratio of formation rates was closer to unity. We also studied the second approximation of Eq. (5), i.e. the decision to use the averaged growth rate of 3–7 nm particles, and found that using a more accurate growth rate of exactly 6 nm particles has an insignificant effect on the value of the formation rate. The remaining approximated quantity in Eq. (5), i.e. the number concentration of 3–6 nm particles, may also be defined more accurately. As opposed to calculating N_{3-6} simply as a sum of particle concentrations in bins within 3–6 nm, a more accurate numerical integration increases the term, and the ratio between the formation rates actually decreases by 7%. In total, using all of the mentioned “improvements” decreases the ratio between the formation rates by 4% in the studied case.

We also tested how the ratio between the formation rates (Eqs. 3 and 5) would change if the particle diameter range in Eq. (5) would be different from 3–6 nm. The results of this analysis are presented in Table 2. Here, all the “improvements” suggested in the previous paragraph were applied, and all occurrences of 6 nm in the modified Eq. (5) were replaced with the new upper limit of the diameter range. Perhaps a bit surprisingly, our sensitivity test suggests that the applied particle diameter range affects the accuracy of J_3 significantly, with a broader range giving greater accuracy, until 3–13 nm, after which the applied Eq. (5) begins to underestimate the formation rate.

A numerical comparison of formation rates

H. Vuollekoski et al.

Title Page

Abstract

Introduction

Conclusions

References

Tables

Figures

⏪

⏩

◀

▶

Back

Close

Full Screen / Esc

Printer-friendly Version

Interactive Discussion



A numerical comparison of formation rates

H. Vuollekoski et al.

Title Page

Abstract

Introduction

Conclusions

References

Tables

Figures

◀

▶

◀

▶

Back

Close

Full Screen / Esc

Printer-friendly Version

Interactive Discussion



Of course, this is caused by a numerical effect due to the significant decrease in the growth rate term in Eq. (5). While bringing the two values of formation rates closer to each other, this effect is unable to explain their difference caused by the coagulation term. Obviously the exact numbers will vary depending on the case: for example, for the case which we used to study the effect of halving the background particle concentration, the maximum ratio occurs with the diameter range of 3–18 nm.

Another factor that could have an effect on the formation rates is the size resolution of the data, or in this case, the number of sections in the model. A brief sensitivity test suggested that a higher size resolution would magnify the difference between the formation rates predicted by Eqs. (3) and (5), but only slightly (cf. Table 1). The effects of numerical diffusion were not considered in this study.

In order to compare the particle formation rates at 2 nm, we performed a brief test on the ratio between Eq. (3) applied at 2 nm and Eq. (5) applied with the diameter range 2–3 nm (Kulmala et al., 2007). The ratio between these two values for J_2 was 0.73 using the “improved” analysis (see above) with the reference data. Scavenging of 2 nm particles is twice as fast as that of 3 nm particles, which is the reason for the increased disagreement between the two formation rates as compared to the J_3 analysis above. As was in the case of J_3 , the ratio increased as upper limit of the diameter range was broadened, reaching unity around 7 nm in the analysed data.

The presented results suggest that most of the deviation between Eqs. (3) and (5) occurs because of coagulation. However, the error rises not from the coagulation term of Eq. (5), but from approximating n_6 by $N_{3-6}/3$ nm, a particle diameter range that is significantly affected by coagulation scavenging. Since the coagulation sink decreases with increasing particle size, a better solution would be estimating n_6 at a larger size, for example

$$J_3 = \frac{\Delta N_{3-6}}{\Delta t} + \text{Coag}S_4 \times N_{3-6} + \frac{\text{GR}_{3-7}}{7 \text{ nm} - 5 \text{ nm}} \times N_{5-7}. \quad (8)$$

The ratio between Eqs. (3) and (8) was found to be 1.06, which could be said to be a significant improvement over the results shown above. Also, if the last term

$GR_{3-7}/2\text{ nm}\times N_{5-7}$ was replaced by J_6 (as calculated from Eq. (3) at 6 nm), the error of J_3 given by Equation 8 was found to be within 1% as compared to Eq. (3). Because this modification is easily implemented in data analysis, we recommend the usage of Eq. (8) over Eq. (5).

Obviously the numbers presented in this section are examples for the studied case, and cannot be used to accurately quantify a systematic error. Nevertheless the trends related to and approximate magnitudes of different phenomena should be general.

4.2 Implications of the varying time delay

If new particle formation is controlled solely by the sulphuric acid concentration, as is the case in the simulations of this study, it should follow from Eq. (6) that the maximum of $[H_2SO_4]$ precedes the maximum of J_3 by a time delay that is associated with the time it takes for particles to grow from the size of the critical clusters (here 1.5 nm) to 3 nm. We performed some analysis on this assumption by calculating the varying time delay using Eq. (7) as suggested by Vuollekoski et al. (2010), and found that the mentioned assumption is inaccurate (see Fig. 5). Otherwise the maximum of the “time-shifted” J_3 should coincide with the maximum of $[H_2SO_4]$, which is clearly not the case. An even more accurate determination of the time delay, as compared with Eq. (7), would not affect its magnitude enough. Therefore, the power-law of Eq. (6) should not be considered an accurate description of the connection between J_3 and $[H_2SO_4]$.

The terms of Eq. (3) are plotted in Fig. 6. In this case, the particles are grown by sulphuric acid and a non-volatile organic vapour of constant concentration. The maximum of growth rate obviously occurs at the same time with the sulphuric acid maximum, and the maximum of $\Delta N/\Delta D_p|_3$ occurs later. The maximum of J_3 , as a product of the two terms in Eq. (3), occurs somewhere in-between. If the particle distribution was continuous, the maximum of the “time-shifted” $\partial N/\partial D_p|_3$ should then coincide with the maximum of $[H_2SO_4]$: maximum nucleation rate is directly transferred to maximum particle size distribution function at a certain size. In a fixed sectional

A numerical comparison of formation rates

H. Vuollekoski et al.

Title Page

Abstract

Introduction

Conclusions

References

Tables

Figures

◀

▶

◀

▶

Back

Close

Full Screen / Esc

Printer-friendly Version

Interactive Discussion



model however, the number concentration of particles in the near-3-nm bin is mixed by numerical diffusion: the formed particles are grown and divided into adjacent bins; some information is lost.

It should be noted that the presense of an additional vapour (with non-constant concentration) participating in growth may decrease the time delay (e.g. Vuollekoski et al., 2010). Additionally, the coagulation sink changes during the day, and this may have an effect on the time delay as well.

5 Summary and conclusions

Different methods of determining formation rates of 3 nm particles were compared. The comparison was based on data analysis performed on output data from a sectional aerosol dynamics model in various cases of differing model parameters. However, the results are valid for experimental discrete particle size distribution analyses as well. The study showed that the method of determining formation rates indirectly from the measured concentration of 3–6 nm particles (Eq. 5, e.g. Sihto et al., 2006) is generally in good agreement with the more accurate Eq. (3) with a systematic error of 0–20% that can mostly be attributed to coagulation. The error is reduced by a few percents if the coagulation sink is calculated more accurately, or if the growth rate is very high, or if the background particle concentration is relatively insignificant. It can therefore be concluded that the general uncertainties related to experimental measurements greatly exceed the error caused by using approximative expressions for formation rate, and both methods are accurate enough in atmospheric applications. Nevertheless, since a partial solution to the error caused by coagulation is easily applied in data analysis, the presented modification (Eq. 8) is recommended.

Additionally, the connection between the concentration of the nucleating vapour and the formation rate was studied. Several studies have found similarities between the temporal behaviours of sulphuric acid concentration and the formation rate (e.g. Sihto et al., 2006; Riipinen et al., 2007; Kuang et al., 2008). Since nucleation is assumed

A numerical comparison of formation rates

H. Vuollekoski et al.

Title Page

Abstract

Introduction

Conclusions

References

Tables

Figures

◀

▶

◀

▶

Back

Close

Full Screen / Esc

Printer-friendly Version

Interactive Discussion



to depend on sulphuric acid, a time delay is associated due to the finite growth rate of particles from their initial size to the observed one. A detailed study showed that this time-shift analysis and the related power-law are inaccurate: the maximum of sulphuric acid concentration does not correspond to the maximum of formation rate, and can occur both before or after it. This has an uncertain effect on the performed “fits” between the two quantities.

Acknowledgements. The financial support by the Academy of Finland Centre of Excellence program (project no. 1118615) is gratefully acknowledged. This work has been partially funded by European Commission 6th Framework programme project EUCAARI, contract no. 036833-2 (EUCAARI).

References

- Aalto, P., Hämeri, K., Becker, E., Weber, R., Salm, J., Mäkelä, J. M., Hoell, C., O’Dowd, C. D., Karlsson, H., Hansson, H., Väkevä, M., Koponen, I., Buzorius, G., and Kulmala, M.: Physical characterization of aerosol particles during nucleation events, *Tellus B*, 53, 344–358, 2001. 18786
- Anttila, T., Kerminen, V.-M., and Lehtinen, K. E. J.: Parameterizing the formation rate of new particles: The effect of nuclei self-coagulation, *J. Aerosol Sci.*, 41, 621–636, doi:10.1016/j.jaerosci.2010.04.008, 2010. 18783, 18785
- Iida, K., Stolzenburg, M. R., and McMurry, P. H.: Effect of Working Fluid on Sub-2 nm Particle Detection with a Laminar Flow Ultrafine Condensation Particle Counter, *Aerosol Sci. Tech.*, 43, 81–96, doi:10.1080/02786820802488194, 2009. 18782
- Kerminen, V.-M. and Kulmala, M.: Analytical formulae connecting the “real” and the “apparent” nucleation rate and the nuclei number concentration for atmospheric nucleation events, *J. Aerosol Sci.*, 33, 609–622, 2002. 18783
- Kerminen, V.-M., Anttila, T., Lehtinen, K. E. J., and Kulmala, M.: Parameterization for atmospheric new-particle formation: Application to a system involving sulfuric acid and condensable water-soluble organic vapors, *Aerosol Sci. Tech.*, 38, 1001–1008, doi:10.1080/027868290519085, 2004. 18783

A numerical comparison of formation rates

H. Vuollekoski et al.

Title Page

Abstract

Introduction

Conclusions

References

Tables

Figures



Back

Close

Full Screen / Esc

Printer-friendly Version

Interactive Discussion



A numerical comparison of formation rates

H. Vuollekoski et al.

Title Page

Abstract

Introduction

Conclusions

References

Tables

Figures

◀

▶

◀

▶

Back

Close

Full Screen / Esc

Printer-friendly Version

Interactive Discussion



Korhonen, H., Lehtinen, K. E. J., and Kulmala, M.: Multicomponent aerosol dynamics model UHMA: model development and validation, *Atmos. Chem. Phys.*, 4, 757–771, doi:10.5194/acp-4-757-2004, 2004. 18786

5 Kuang, C., McMurry, P., McCormick, A., and Eisele, F.: Dependence of nucleation rates on sulfuric acid vapor concentration in diverse atmospheric locations, *J. Geophys. Res.-Atmos.*, 113, D10209, doi:10.1029/2007JD009253, 2008. 18788, 18793

Kulmala, M. and Kerminen, V.-M.: On the formation and growth of atmospheric nanoparticles, *Atmos. Res.*, 90, 132–150, doi:10.1016/j.atmosres.2008.01.005, 2008. 18782

10 Kulmala, M., Dal Maso, M., Mäkelä, J., Pirjola, L., Väkevä, M., Aalto, P., Miikkulainen, P., Hameri, K., and O'Dowd, C.: On the formation, growth and composition of nucleation mode particles, *Tellus B*, 53, 479–490, 2001. 18787

Kulmala, M., Vehkamäki, H., Petäjä, T., Dal Maso, M., Lauri, A., Kerminen, V.-M., Birmili, W., and McMurry, P.: Formation and growth rates of ultrafine atmospheric particles: a review of observations, *J. Aerosol Sci.*, 35, 143–176, doi:10.1016/j.jaerosci.2003.10.003, 2004. 18782

15 Kulmala, M., Lehtinen, K. E. J., and Laaksonen, A.: Cluster activation theory as an explanation of the linear dependence between formation rate of 3nm particles and sulphuric acid concentration, *Atmos. Chem. Phys.*, 6, 787–793, doi:10.5194/acp-6-787-2006, 2006. 18786, 18788, 18789

20 Kulmala, M., Riipinen, I., Sipilä, M., Manninen, H., Petäjä, T., Junninen, H., Dal Maso, M., Mordas, G., Mirme, A., Vana, M., Hirsikko, A., Laakso, L., Harrison, R., Hanson, I., Leung, C., Lehtinen, K. E. J., and Kerminen, V.-M.: Toward direct measurement of atmospheric nucleation, *Science*, 318, 89–92, doi:10.1126/science.1144124, 2007. 18782, 18784, 18791

25 Lehtinen, K. E. J., Dal Maso, M., Kulmala, M., and Kerminen, V.-M.: Estimating nucleation rates from apparent particle formation rates and vice versa: Revised formulation of the Kerminen-Kulmala equation, *J. Aerosol Sci.*, 38, 988–994, doi:10.1016/j.jaerosci.2007.06.009, 2007. 18783

Lehtipalo, K., Sipilä, M., Riipinen, I., Nieminen, T., and Kulmala, M.: Analysis of atmospheric neutral and charged molecular clusters in boreal forest using pulse-height CPC, *Atmos. Chem. Phys.*, 9, 4177–4184, doi:10.5194/acp-9-4177-2009, 2009. 18782

30 Makkonen, R., Asmi, A., Korhonen, H., Kokkola, H., Järvenoja, S., Räisänen, P., Lehtinen, K. E. J., Laaksonen, A., Kerminen, V.-M., Järvinen, H., Lohmann, U., Bennartz, R., Feichter, J., and Kulmala, M.: Sensitivity of aerosol concentrations and cloud properties to nucleation and secondary organic distribution in ECHAM5-HAM global circulation model, *Atmos. Chem.*

A numerical comparison of formation rates

H. Vuollekoski et al.

Title Page

Abstract

Introduction

Conclusions

References

Tables

Figures

◀

▶

◀

▶

Back

Close

Full Screen / Esc

Printer-friendly Version

Interactive Discussion



Phys., 9, 1747–1766, doi:10.5194/acp-9-1747-2009, 2009. 18782

Manninen, H., Petäjä, T., Asmi, E., Riipinen, I., Nieminen, T., Mikkilä, J., Hörrak, U., Mirme, A., Mirme, S., Laakso, L., Kerminen, V.-M., and Kulmala, M.: Long-term field measurements of charged and neutral clusters using Neutral cluster and Air Ion Spectrometer (NAIS), Boreal Environ. Res., 14, 591–605, 2009. 18782, 18784

McMurry, P. and Friedlander, S.: New particle formation in the presence of an aerosol, Atmos. Environ., 13, 1635–1651, 1979. 18788

McMurry, P. H., Fink, M., Sakurai, H., Stolzenburg, M. R., Mauldin, R. L., Smith, J., Eisele, F., Moore, K., Sjostedt, S., Tanner, D., Huey, L. G., Nowak, J. B., Edgerton, E., and Voisin, D.: A criterion for new particle formation in the sulfur-rich Atlanta atmosphere, J. Geophys. Res.-Atmos., 110, D22S02, doi:10.1029/2005JD005901, 2005. 18783

Merikanto, J., Spracklen, D. V., Mann, G. W., Pickering, S. J., and Carslaw, K. S.: Impact of nucleation on global CCN, Atmos. Chem. Phys., 9, 8601–8616, doi:10.5194/acp-9-8601-2009, 2009. 18782

Metzger, A., Verheggen, B., Dommen, J., Duplissy, J., Prevot, A., Weingartner, E., Riipinen, I., Kulmala, M., Spracklen, D., Carslaw, K., and Baltensperger, U.: Evidence for the role of organics in aerosol particle formation under atmospheric conditions, P. Natl. Acad. Sci. USA, 107, 6646–6651, doi:10.1073/pnas.0911330107, 2010. 18788

Paasonen, P., Sihto, S.-L., Nieminen, T., Vuollekoski, H., Riipinen, I., Plass-Dülmer, C., Berresheim, H., Birmili, W., and Kulmala, M.: Connection between new particle formation and sulphuric acid at Hohenpeissenberg (Germany) including the influence of organic compounds, Boreal Environ. Res., 14, 616–629, 2009. 18788

Paasonen, P., Nieminen, T., Asmi, E., Manninen, H. E., Petäjä, T., Plass-Dülmer, C., Flentje, H., Birmili, W., Wiedensohler, A., Hörrak, U., Metzger, A., Hamed, A., Laaksonen, A., Facchini, M. C., Kerminen, V.-M., and Kulmala, M.: On the roles of sulphuric acid and low-volatility organic vapours in the initial steps of atmospheric new particle formation, Atmos. Chem. Phys. Discuss., 10, 11795–11850, doi:10.5194/acpd-10-11795-2010, 2010. 18788

Pierce, J. R. and Adams, P. J.: Uncertainty in global CCN concentrations from uncertain aerosol nucleation and primary emission rates, Atmos. Chem. Phys., 9, 1339–1356, doi:10.5194/acp-9-1339-2009, 2009. 18782

Riipinen, I., Sihto, S.-L., Kulmala, M., Arnold, F., Dal Maso, M., Birmili, W., Saarnio, K., Teinilä, K., Kerminen, V.-M., Laaksonen, A., and Lehtinen, K. E. J.: Connections between atmospheric sulphuric acid and new particle formation during QUEST IIIIV campaigns in Heidel-

A numerical comparison of formation rates

H. Vuollekoski et al.

Title Page

Abstract

Introduction

Conclusions

References

Tables

Figures

◀

▶

◀

▶

Back

Close

Full Screen / Esc

Printer-friendly Version

Interactive Discussion



berg and Hyytiälä, Atmos. Chem. Phys., 7, 1899–1914, doi:10.5194/acp-7-1899-2007, 2007. 18787, 18788, 18793

Seinfeld, J. H. and Pandis, S. N.: Atmospheric Chemistry and Physics, Wiley, 2006. 18784

Sihto, S.-L., Kulmala, M., Kerminen, V.-M., Dal Maso, M., Petäjä, T., Riipinen, I., Korhonen, H.,
5 Arnold, F., Janson, R., Boy, M., Laaksonen, A., and Lehtinen, K. E. J.: Atmospheric sulphuric
acid and aerosol formation: implications from atmospheric measurements for nucleation and
early growth mechanisms, Atmos. Chem. Phys., 6, 4079–4091, doi:10.5194/acp-6-4079-
2006, 2006. 18787, 18788, 18793

Sipilä, M., Lehtipalo, K., Kulmala, M., Petäjä, T., Junninen, H., Aalto, P. P., Manninen, H. E.,
10 Kyrö, E.-M., Asmi, E., Riipinen, I., Curtius, J., Kürten, A., Borrmann, S., and O'Dowd, C.
D.: Applicability of condensation particle counters to measure atmospheric clusters, Atmos.
Chem. Phys., 8, 4049–4060, doi:10.5194/acp-8-4049-2008, 2008. 18782

Sipilä, M., Berndt, T., Petäjä, T., Brus, D., Vanhanen, J., Stratmann, F., Patokoski, J., Mauldin,
15 R., Hyvärinen, A., Lihavainen, H., and Kulmala, M.: The Role of Sulfuric Acid in Atmospheric
Nucleation, Science, 327, 1243–1246, doi:10.1126/science.1180315, 2010. 18788

Spracklen, D. V., Carslaw, K. S., Kulmala, M., Kerminen, V.-M., Mann, G. W., and Sihto, S.-
L.: The contribution of boundary layer nucleation events to total particle concentrations on
regional and global scales, Atmos. Chem. Phys., 6, 5631–5648, doi:10.5194/acp-6-5631-
2006, 2006. 18782

20 Spracklen, D., Carslaw, K., Kulmala, M., Kerminen, V.-M., Sihto, S.-L., Riipinen, I., Merikanto, J.,
Mann, G., Chipperfield, M., Wiedensohler, A., Birmili, W., and Lihavainen, H.: Contribution of
particle formation to global cloud condensation nuclei concentrations, Geophys. Res. Lett.,
35, L06808, doi:10.1029/2007GL033038, 2008. 18782

Vuollekoski, H., Nieminen, T., Paasonen, P., Sihto, S.-L., Boy, M., Manninen, H. E., Lehtinen, K.
25 E. J., Kerminen, V.-M., and Kulmala, M.: Atmospheric nucleation and initial steps of particle
growth: numerical comparison of different theories and hypotheses, Atmos. Res., in press,
2010. 18788, 18792, 18793

Weber, R., Marti, J., McMurry, P., Eisele, F., Tanner, D., and Jefferson, A.: Measured atmo-
spheric new particle formation rates: Implications for nucleation mechanisms, Chemical En-
30 gineering Communications, 151, 53–64, 1996. 18787

Yu, F. and Luo, G.: Simulation of particle size distribution with a global aerosol model: con-
tribution of nucleation to aerosol and CCN number concentrations, Atmos. Chem. Phys., 9,
7691–7710, doi:10.5194/acp-9-7691-2009, 2009. 18782

A numerical comparison of formation rates

H. Vuollekoski et al.

Title Page

Abstract

Introduction

Conclusions

References

Tables

Figures

◀

▶

◀

▶

Back

Close

Full Screen / Esc

Printer-friendly Version

Interactive Discussion



Table 1. Sensitivity of the ratio of formation rates (Eq. 3/Eq. 5, calculated as a mean of values during 11:00–13:00) to different parameters affecting new particle formation. Nomenclature: BKG=background particle concentration, A =activation coefficient, bins=number of size sections.

Varied parameter	Ratio
none	0.87
BKG \rightarrow 0	1.00
BKG \rightarrow $\frac{1}{10}$ \times BKG	0.96
BKG \rightarrow $\frac{1}{2}$ \times BKG	0.91
BKG \rightarrow 4 \times BKG	0.84
$A \rightarrow$ $\frac{1}{4}$ \times A	0.87
$A \rightarrow$ 4 \times A	0.87
GR ₃₋₇ \rightarrow 0.77 \times GR ₃₋₇	0.78
GR ₃₋₇ \rightarrow 1.9 \times GR ₃₋₇	0.97
bins \rightarrow $\frac{2}{3}$ \times bins	0.89
bins \rightarrow 2.5 \times bins	0.85

A numerical comparison of formation rates

H. Vuollekoski et al.

Table 2. Sensitivity of the ratio of formation rates (Eq. 3/Eq. 5, calculated as a mean of values during 11:00–13:00) to modifications and improvements in analysis. The first three improvements are included in all the latter ones (applied at the respective size range).

Modification of Analysis	Ratio
none	0.87
CoagS ₄ → CoagS _{3–6}	0.91
GR _{3–7} → GR ₆	0.86
more accurate N _{3–6}	0.80
all of the above	0.83
using 3–4 nm range	0.80
using 3–7 nm range	0.84
using 3–10 nm range	0.92
using 3–13 nm range	1.00
using 3–15 nm range	1.06
using 3–25 nm range	1.41
N _{3–6} /3 nm → N _{5–7} /2 nm	1.06

Title Page

Abstract

Introduction

Conclusions

References

Tables

Figures

◀

▶

◀

▶

Back

Close

Full Screen / Esc

Printer-friendly Version

Interactive Discussion



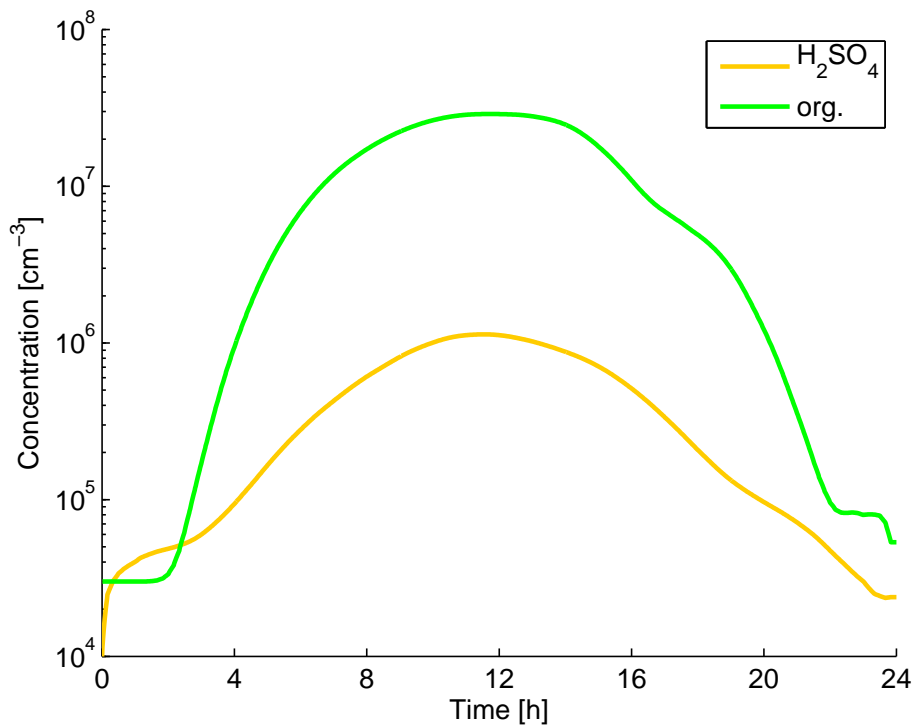


Fig. 1. The concentrations of sulphuric acid and a non-volatile organic vapour used in the simulations.

A numerical comparison of formation rates

H. Vuollekoski et al.

Title Page

Abstract Introduction

Conclusions References

Tables Figures

◀ ▶

◀ ▶

Back Close

Full Screen / Esc

Printer-friendly Version

Interactive Discussion



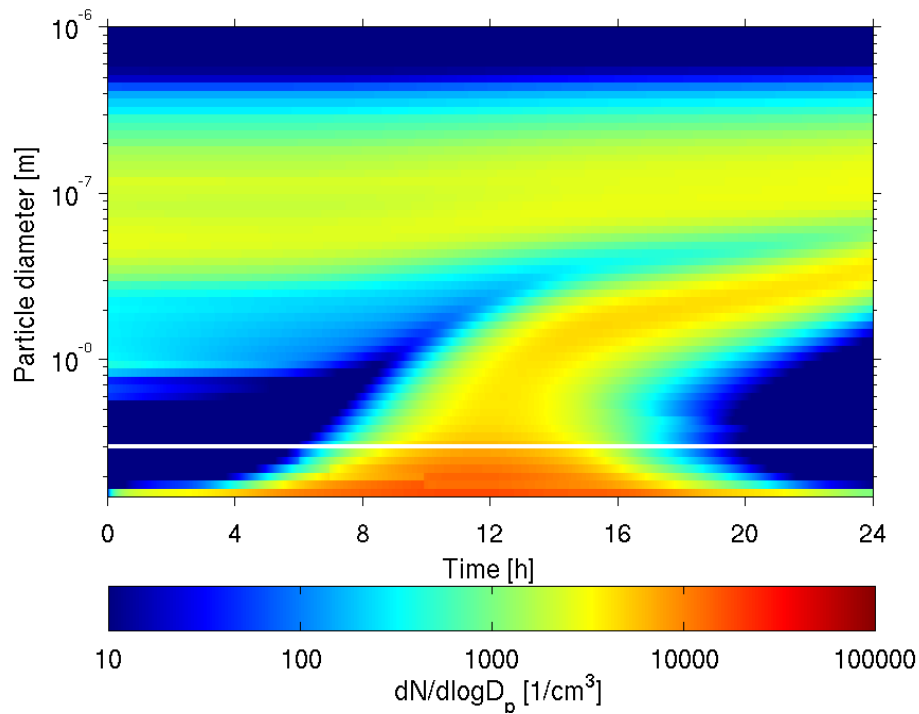


Fig. 2. The simulated particle size distribution data used in the analysis.

A numerical comparison of formation rates

H. Vuollekoski et al.

Title Page

Abstract Introduction

Conclusions References

Tables Figures

◀ ▶

◀ ▶

Back Close

Full Screen / Esc

Printer-friendly Version

Interactive Discussion



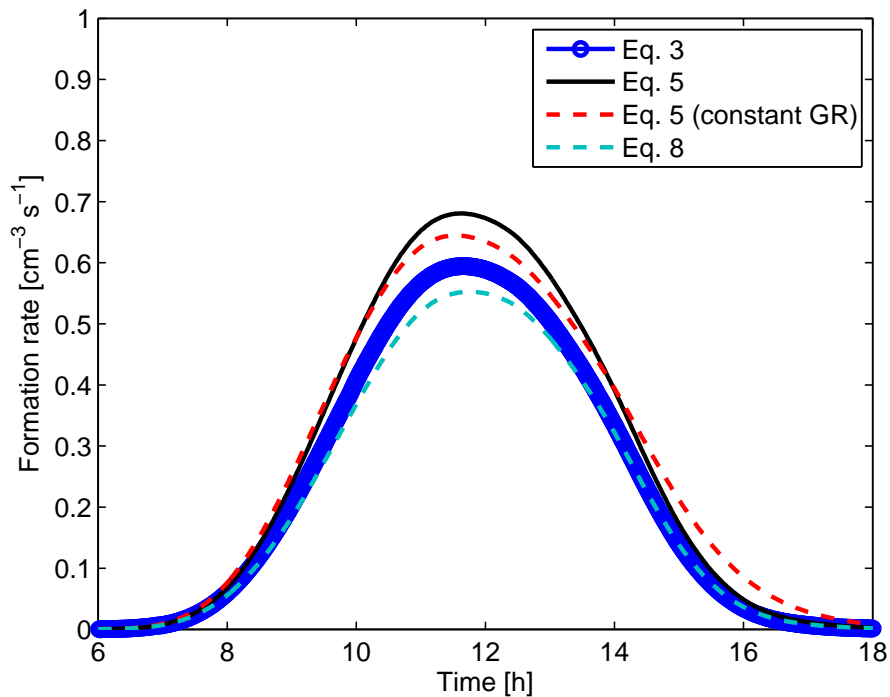


Fig. 3. Comparison of formation rates calculated using different methods during a simulated new particle formation event.

A numerical comparison of formation rates

H. Vuollekoski et al.

Title Page

Abstract Introduction

Conclusions References

Tables Figures

◀ ▶

◀ ▶

Back Close

Full Screen / Esc

Printer-friendly Version

Interactive Discussion



A numerical comparison of formation rates

H. Vuollekoski et al.

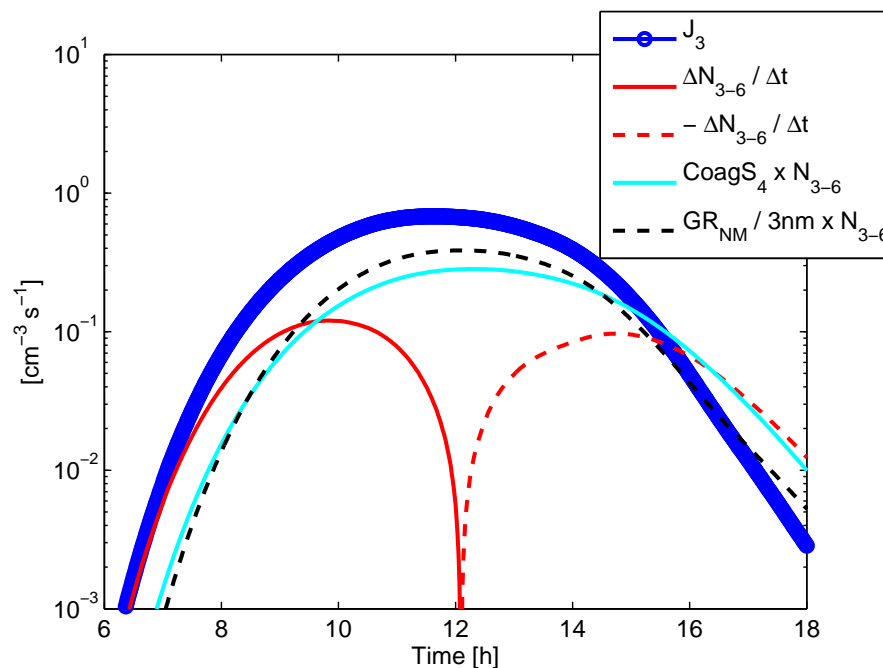


Fig. 4. Comparison of different terms contributing to the Eq. (3) for formation rate. The positive and negative parts of the $\Delta N_{3-6}/\Delta t$ term are plotted separately.

Title Page

Abstract

Introduction

Conclusions

References

Tables

Figures

◀

▶

◀

▶

Back

Close

Full Screen / Esc

Printer-friendly Version

Interactive Discussion



**A numerical
comparison of
formation rates**

H. Vuollekoski et al.

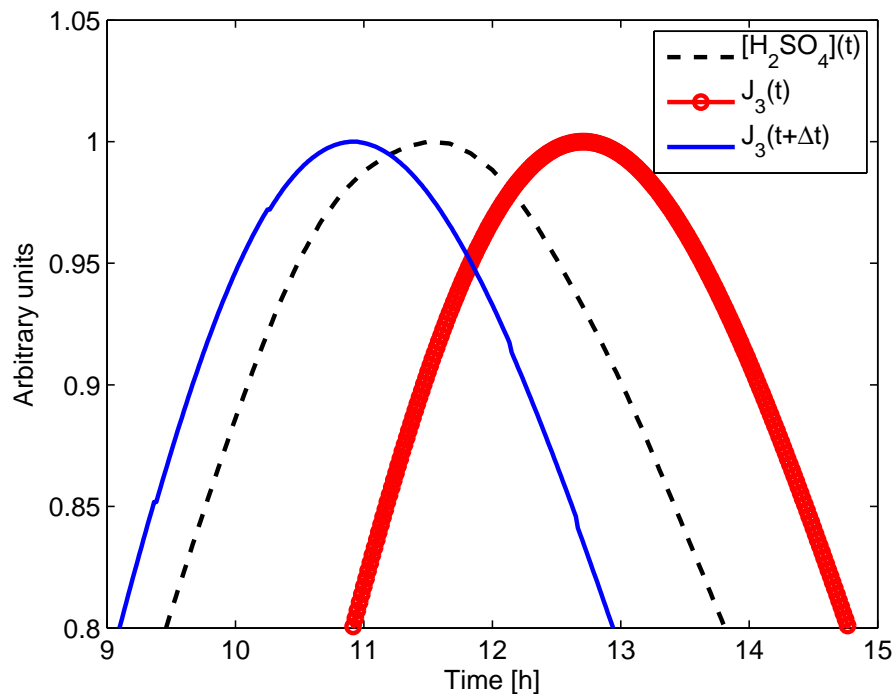


Fig. 5. Temporal behaviour of the sulphuric acid concentration, the formation rate J_3 and the same as time-shifted by the time delay (Eq. 7) near sulphuric acid concentration maximum.

Title Page

Abstract

Introduction

Conclusions

References

Tables

Figures

◀

▶

◀

▶

Back

Close

Full Screen / Esc

Printer-friendly Version

Interactive Discussion



**A numerical
comparison of
formation rates**

H. Vuollekoski et al.

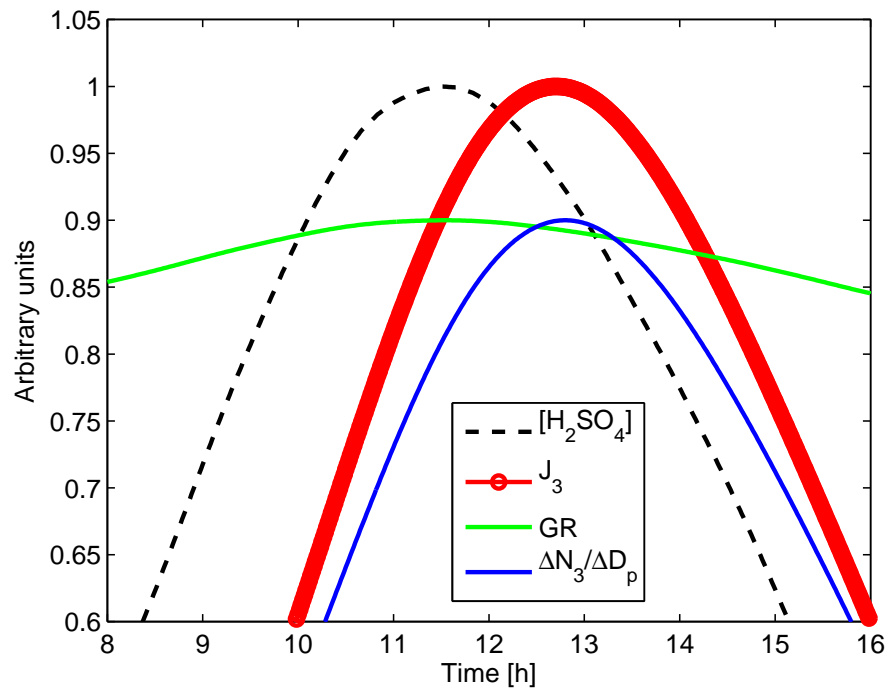


Fig. 6. Temporal behaviour of different quantities contributing to the formation rate.

Title Page

Abstract

Introduction

Conclusions

References

Tables

Figures

◀

▶

◀

▶

Back

Close

Full Screen / Esc

Printer-friendly Version

Interactive Discussion

